Spin-state responses to light impurity substitution in low-spin perovskite LaCoO₃

Keisuke Tomiyasu,[1,*] Yuuki Kubota,[1] Saya Shimomura,[1] Mitsugi Onodera,[1] Syun-Ichi Koyama,[1] Tsutomu Nojima,[2] Sumio Ishihara,[1] Hironori Nakao,[3,4] and Youichi Murakami[3]

[1]*Department of Physics, Tohoku University, Aoba, Sendai 980-8578, Japan*

[2]*Institute for Materials Research, Tohoku University, Aoba, Sendai 980-8577, Japan*

[3]*Condensed Matter Research Center and Photon Factory, Institute of Materials Structure Science,*
High Energy Accelerator Research Organization, Tsukuba, Ibaraki 305-0801, Japan

[4]*CREST, Japan Science and Technology Agency (JST), Tokyo, 102-0076 Japan*

We studied the spin-state responses to light impurity substitution in low-spin perovskite LaCoO₃ (Co^{3+}: d^6) through magnetization, x-ray fluorescence, and electrical resistivity measurements of single-crystal $LaCo_{0.99}M_{0.01}O_3$ (M = Cr, Mn, Fe, Ni). In the magnetization curves measured at 1.8 K, a change in the spin-state was not observed for Cr, Mn, or Fe substitution but was observed for Ni substitution. Strong magnetic anisotropy was also found in the Ni-substituted sample. The fluorescence measurements revealed that the valences were roughly estimated to be Cr^{3+}, $Mn^{(4-\delta)+}$, $Fe^{(3+\delta')+}$, and Ni^{3+}. From the observed chemical trends, we propose that the chemical potential is a key factor in inducing the change of the low-spin state. By expanding a model of the ferromagnetic spin-state heptamer generated by hole doping [Podlesnyak *et al.*, Phys. Rev. Lett. **101**, 247603 (2008)], the emergence of highly *anisotropic* spin-state molecular ferromagnets induced by low-spin Ni^{3+} with Jahn-Teller activity is suggested. We also discuss applicability of the present results to other materials with Fe (d^6).

I. INTRODUCTION

Transition-metal oxides have been found to exhibit exotic electronic phenomena such as colossal magnetic resistivity and high-T_c superconductivity, which are based on the strong correlations among the spin, orbital, charge, and lattice. In particular, perovskite-type cobalt oxide LaCoO₃ (Co^{3+}: d^6) is a rare inorganic material with spin-state degrees of freedom: low-spin (LS), intermediate-spin (IS), and high-spin (HS) states, as shown in Fig. 1(a).[1–5] The Co^{3+} ion is surrounded octahedrally by six O^{2-} ions, and the crystal field splits the fivefold d orbitals into triply degenerate t_{2g} (d_{xy}, d_{yz}, d_{zx}) orbitals with a lower energy and doubly degenerate e_g ($d_{3z^2-r^2}$, $d_{x^2-y^2}$) orbitals with a higher energy. The LS (HS) state appears when the crystal-field splitting energy is larger (smaller) than the Hund coupling energy, while the IS state is also theoretically possible through hybridization of the Co 3d (e_g) and O 2p orbitals when these energies are similar.[6]

LaCoO₃ exhibits insulating nonmagnetic LS states below about 20 K,[1–3] and as the temperature increases, the LS states gradually change to homogeneous magnetic IS states or inhomogeneous states of LS and magnetic HS with semiconductivity towards about 100 K. Further change to homogeneous HS states with metallic conductivity occurs around 600 K. LaCoO₃ therefore exhibits temperature-induced spin-state transitions.[1–3] Such a spin-state transition can also be induced by a high magnetic field[4] and by a high pressure.[5] Thus, these sensitive responses of the spin states demonstrate their near degeneracy in energy.

LaCoO₃ in an LS state also displays striking and fascinating responses to impurity substitution. For example, very light Sr^{2+} substitution (below 1%) of the La^{3+} sites, which corresponds to hole doping from Co^{3+} to Co^{4+}, generates a large magnetic moment of over 10 μ_B/hole, significantly

larger than the maximum value of 5 μ_B in d electron systems.[7] Further Sr substitution leads to ferromagnetic spin glass, colossal magnetic resistivity, the anomalous Hall effect, and an insulator-to-metal transition.[8] In addition, Mn and Ni substitution of the Co sites induces colossal magnetic resistivity, an insulator-to-metal transition, and ferromagnetic semi-conductivity with a high Curie temperature.[9,10] Both Mn- and Ni-substituted LaCoO₃ are expected to be used in thin-film applications.[11] Moreover, Co-site Fe substitution induces weak ferromagnetism and a large magnetic anisotropy.[12–14]

The Sr-substitution phenomena were proposed[15–17] and established[18,19] to microscopically originate from ferromagnetic spin-state polarons, which refer to spin clusters consisting of a core radical Co^{4+} ion and its surrounding magnetic-spin-state Co^{3+} ions changing from the LS state.[20] The driving force is thought to be the double exchange interactions between Co^{3+} and Co^{4+}; an electron is excited from the t_{2g} to e_g orbital in Co^{3+} (LS to IS) and then hops between the Co^{3+} and Co^{4+} e_g orbitals.[15,16] In inelastic neutron scattering studies for 0.2% to 1% Sr substitution, the best fit of the scattering vector (Q) dependence of the intensities is provided by a spin heptamer model with a core radical Co^{4+} ion and six nearest-neighbor Co^{3+} ions (IS).[18,19] Pure isolated polarons are observed only for substitution levels below 1%, and the system enters the ferromagnetic spin glass phase owing to interpolaron interactions at a substitution level of at least 2%.[19,21,22]

Based on the double exchange mechanism, Co-site substituted $LaCo_{1-y}M_yO_3$ should also generate similar spin-state polarons when at least one majority-spin e_g orbital is unfilled in the M ions. Indeed, for $M = Ni^{3+}$ (LS) with an unfilled e_g orbital, powder magnetization measurements revealed that Co^{3+} ions change to a magnetic spin state with ferromagnetic correlations at $y \geqslant 0.01$.[10] For $M = Fe^{3+}$ with filled e_g orbitals, powder magnetization measurements,
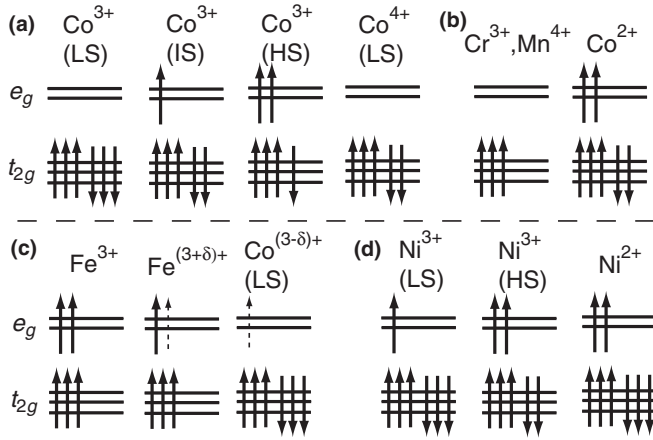
FIG. 1. Schematic diagrams of the t_{2g} and e_g orbital occupations for the 3d transition metal ions in LaCoO$_3$. The up and down arrows indicate up and down spins, respectively. The dotted up arrows express partial occupation of either e_g orbital corresponding to δ.

neutron diffraction, and Mössbauer spectroscopy all indicated that the magnetic properties could be explained only by Fe^{3+} magnetic moments without a spin-state change of Co^{3+} at $y \geqslant 0.15$.[12–14] However, for $M = $ Cr^{3+} with an unfilled e_g orbital, powder magnetization and neutron diffraction studies suggested that the Co^{3+} LS state is maintained at $y \geqslant 0.1$.[23] For $M = $ Mn with an unfilled e_g orbital, x-ray absorption spectroscopy studies for Mn substitution of over 20% revealed that averagely Mn$^{(4-\delta)+}$ and Co$^{(2+\delta)+}$ (electron doping) are generated, and powder magnetization studies suggested that magnetism arises from them coupled by a double exchange interaction without magnetic-spin-state Co^{3+}.[9,24] The extent of δ depends on the substitution level, is estimated to be 0.2 in the extrapolation to zero Mn concentration, and mixed valence of Mn^{3+}/Mn^{4+} and Co^{3+}/Co^{2+} was suggested in the whole substitution range.[9,24]

To explain this spin-state behavior by analogy with the studies of very lightly hole-doped systems,[7,18] it is necessary to minimize the interactions between impurity atoms and impurity contamination in the system and to experimentally reinvestigate the perturbative influence of an isolated impurity atom embedded in the Co^{3+} (LS) matrix. Thus, we performed a comparative study of single crystals of LaCo$_{0.99}M_{0.01}$O$_3$ ($M = $ Cr, Mn, Fe, Ni) with the same low concentration by conducting magnetization, x-ray fluorescence, and electrical resistivity measurements, which have not been investigated thus far. Through these experiments we can determine whether the Co^{3+} LS state changes for each M atom, and for Ni substitution, strong magnetic anisotropy is found for the first time. We discuss another key factor in the change of the Co^{3+} LS state in addition to the double exchange mechanism. We also discuss applicability of the present results to other materials with Fe (d^6).

II. EXPERIMENTS

Single-crystal rods approximately 6 mm in diameter of LaCoO$_3$ and LaCo$_{0.99}M_{0.01}$O$_3$ ($M = $ Cr, Mn, Fe, Ni) were grown in O$_2$ gas flow using the floating-zone method. La$_2$O$_3$, Co$_3$O$_4$, and M_2O$_3$ ($M = $ Cr, Mn, Fe, Ni) powders were

used as the starting materials. In the powder specimens obtained by grinding a piece of the crystal, no reflections other than those of the perovskite structure were observed in the x-ray diffraction patterns. The composition ratios of the metal elements were evaluated by inductively coupled plasma (ICP); La:Co = 1:0.97 for the nonsubstituted sample, La:Co:M = 1:0.96:0.01 for the Cr-, Mn-, and Fe-substituted samples, and 1:0.96:0.009 for the Ni-substituted sample. The number of occupied B sites decreased slightly but the total B-site occupation was constant at 0.97 without any relative differences. In addition, the oxygen defect concentration d defined by ABO_{3-d} was evaluated by thermogravimetry: d was 0.00 ± 0.03, 0.02 ± 0.03, 0.01 ± 0.03, 0.02 ± 0.03, and 0.01 ± 0.03 for the nonsubstituted sample and the Cr-, Mn-, Fe-, and Ni-substituted samples, respectively, which are equivalent within the error range. Thus, these composition evaluations indicate that direct comparisons among these samples is meaningful.

Direct-current magnetization measurements were performed with standard superconducting quantum interference device (SQUID) magnetometers at the Center for Low Temperature Science, Tohoku University, and crystal orientations were determined by x-ray Laue diffraction. Single-crystal specimens of approximately 5 mm^3 were cut from the rods using a diamond disk cutter, fixed on a thin aluminum plate with varnish, and inserted into the magnetometers. X-ray fluorescence measurements were performed at room temperature on the BL-3A and BL-4C beamlines at the Photon Factory at KEK (Japan). To effectively extract the weak signals from the 1% M impurity atoms, the incident x-ray energies were varied around the K-absorption edges of each M atom, and the final energies were also fixed at each K_α energy with an energy-selective detector. Polycrystalline pellets of LaCrO$_3$, LaMnO$_3$, LaFeO$_3$, and (LaSr)NiO$_4$ with M^{3+} synthesized by a standard solid-state reaction method were used for the reference samples. Direct-current electrical resistivity measurements were performed using a standard four-probe method.

III. RESULTS

Figure 2 shows the temperature dependence of the magnetic susceptibility. All the substituted samples exhibit much a larger increase in the susceptibility than the nonsubstituted sample with decreasing temperature, indicating the appearance of a finite magnetic moment as a result of light substitution. Furthermore, no difference between the zero-field-cooling and field-cooling curves was observed, indicating that there are no spin-glass-like components and that magnetic interactions among the impurity atoms in the samples have been minimized.

Figures 3(a)–3(d) show the magnetization curves measured at 1.8 K. The Cr-substituted sample curves are isotropic and follow the $S = 3/2$ Brillouin function [Fig. 3(a)]. The Mn-substituted sample curves are anisotropic, and the magnetic moment is $\sim$7 μ_B at 7 T [Fig. 3(b)]. The Fe-substituted sample curves are slightly anisotropic but mainly follow the $S = 5/2$ Brillouin function [Fig. 3(c)]. Only the Ni-substituted sample curves show a large anisotropy [Fig. 3(d)], and the magnetic moment is $\sim$6 μ_B at 7 T.
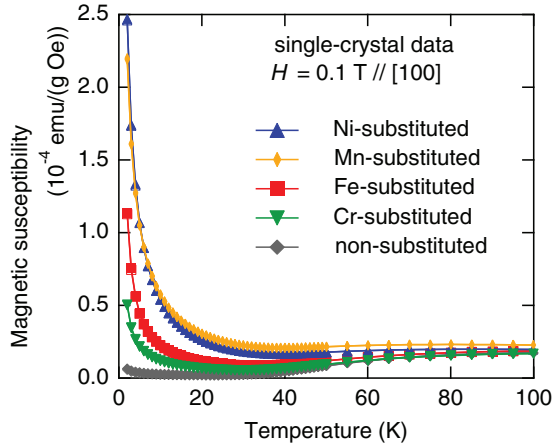
FIG. 2. (Color online) Temperature dependence of the magnetic susceptibility in a magnetic field of 0.1 T applied along the [100] direction. The zero-field-cooling and field-cooling data with errors are of the same size as the symbols.

Figures 4(a)–4(d) show comparisons of the x-ray fluorescence spectra measured at room temperature of the 1%-substituted samples and the trivalent reference samples. In Fig. 4(a), the K-absorption edge positions are nearly equal, indicating that the substituted Cr ion is trivalent. In Fig. 4(b), the edge position remarkably shifts to a higher energy relative

to the reference edge, indicating that the Mn impurity ion is close to tetravalent, $Mn^{(4-\delta)+}$. The extent of this shift (3.0 eV) is consistent with the extrapolation from over $y = 0.2$ to $y = 0.01$ Mn substitution, corresponding to $\delta \sim 0.2$, that is, the mixed valence of 80% Mn^{4+}/20% Mn^{3+}.[24] In Fig. 4(c), the edge position also shifts to a higher energy, indicating that the Fe impurity ion tends toward being tetravalent, $Fe^{(3+\delta')+}$. However, Mössbauer spectroscopy determined the Fe valence to be trivalent for $LaCo_{0.42}Fe_{0.58}O_3$,[14] suggesting that this valence shift appears only at low Fe concentrations. In Fig. 4(d), the edge positions are nearly equal, and so the Ni impurity ion is roughly trivalent.

Figure 5 shows the temperature dependence of the electrical resistivity. As the temperature decreases, the nonsubstituted sample resistivity exhibits exponential increase with a shoulder structure around 80 K, which is accompanied with the spin crossover to nonmagnetic LS state.[25] By contrast, the other substituted ones increase without the shoulder, which coincides with the appearance of a finite magnetic moment, as shown in Fig. 2. All the samples are highly insulating below 30 K, which therefore indicates that, in the low-temperature region in the Mn- and Fe-substituted samples, the doped electron is not itinerant but localized probably around $Mn^{(4-\delta)+}$ and $Fe^{(3+\delta')+}$ by Coulomb attractive force between the electron and the positive ions. Also, in comparison with the nonsubstituted one, the Fe- and Cr-substituted ones are relatively high, and the Mn-substituted
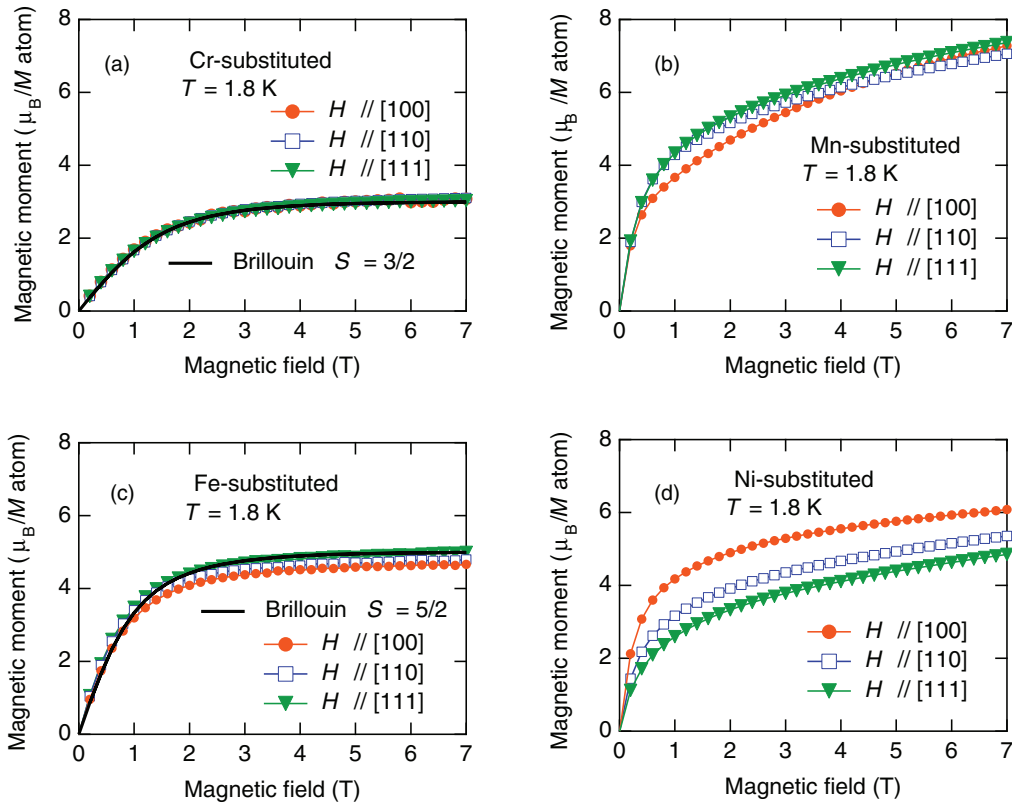

FIG. 3. (Color online) Magnetization curves measured at 1.8 K with increasing magnetic field for the (a) Cr-, (b) Mn-, (c) Fe-, and (d) Ni-substituted samples, respectively. To extract only the magnetization components generated by substitution, the data of the nonsubstituted sample were subtracted from the substituted-sample data. The magnetic field was applied along the [100], [110], and [111] directions in all cases. In (a) and (c), Brillouin functions of $S = 3/2$ and $5/2$ are also shown without any fitting parameter.
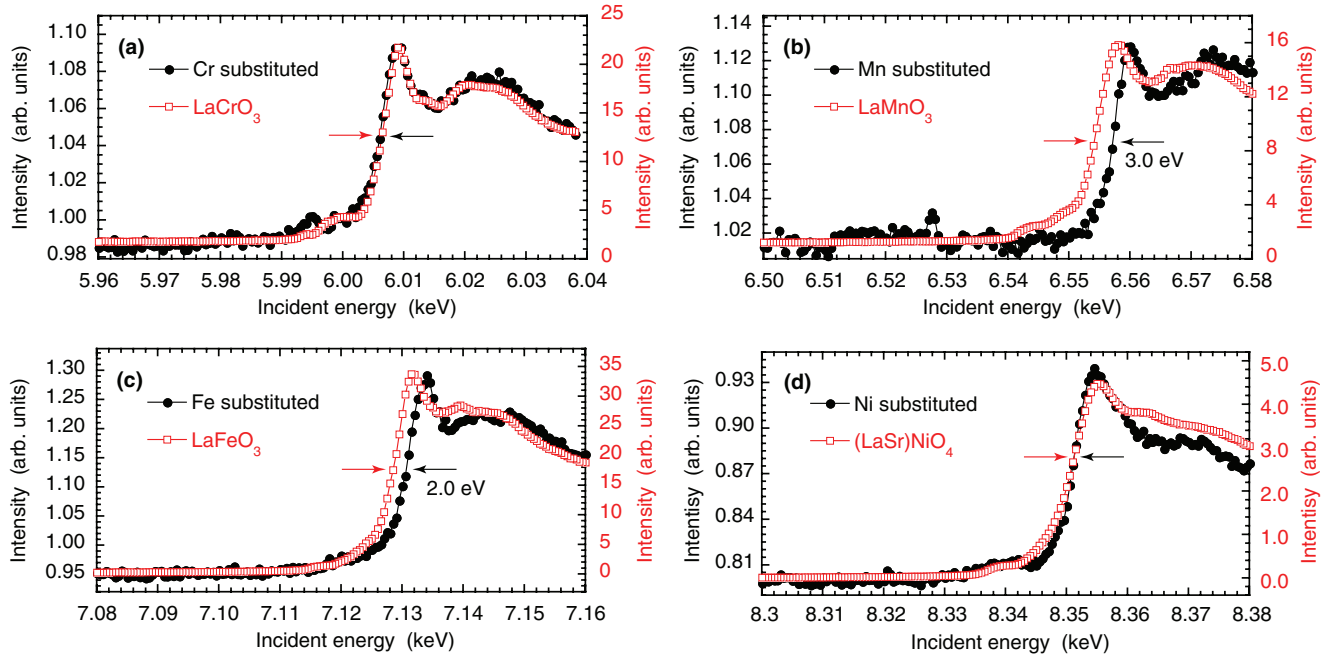
FIG. 4. (Color online) X-ray fluorescence data measured at room temperature for the (a) Cr-, (b) Mn-, (c) Fe-, and (d) Ni-substituted samples (solid black circles) compared with the data for the corresponding reference samples with their trivalent ions (open red squares). The arrow pairs denote the difference in the K absorption edge positions defined as the inflection points. The lines are a guide for the eye. The statistical errors are smaller than the symbol sizes.

one is close until around 100 K but is also high below the temperature.

On the other hand, the Ni-substituted one is considerably lower than the nonsubstituted one in electrical resistivity. This is regarded as the way to the insulator-to-metal transition occurring at 40% Ni concentration.[10] Interestingly, however, the resistivity exhibits extremely rapid decrease with increasing Ni concentration only below a few percent.[10] The low-concentration region is not well understood yet, but the strong magnetic anisotropy presently found (Fig. 3) is expected to link to it. A future study of anisotropy in electrical and magnetic resistivity will provide key information.
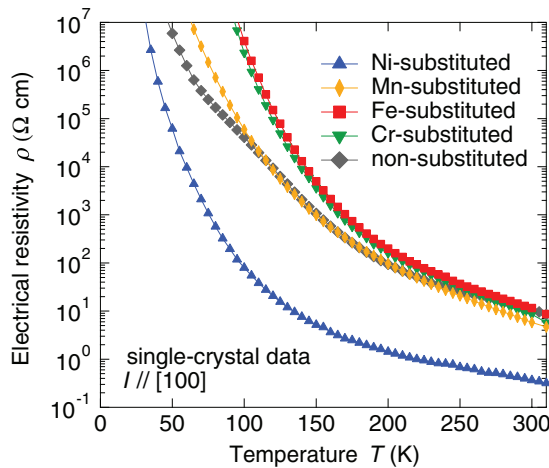

FIG. 5. (Color online) Temperature dependence of the electrical resistivity for a direct current applied along the [100] direction.

IV. DISCUSSION

A. Cr, Mn, and Fe substitution

The results of the magnetization and fluorescence measurements demonstrate that the nonmagnetic LS state of Co^{3+} is robust against Cr^{3+} substitution.

For Mn substitution, since the dominant valence state Mn^{4+} is equivalent to Cr^{3+} in terms of d^3, the Mn^{4+} ion is expected to exhibit similar isotropic magnetization curves to those of Cr^{3+}. The doped electron, that is, the paired Co^{2+} (d^7: $S = 3/2$, effective orbital angular momentum $l = 1$) is expected to exhibit a total moment of $\sim 4\ \mu_B$ with magnetic anisotropy owing to the S and l combination, as in CoO,[27] to which the observed anisotropy is attributed. Further, a ferromagnetic superexchange interaction is expected between Mn^{4+}-O-Co^{2+} in the Goodenough-Kanamori rule,[28] and the ferromagnetic summation of them alone gives a moment of $\sim 7\ \mu_B$, which is in agreement with the present experimental value at 7 T [Fig. 3(b)]. All these facts can be explained without the magnetic-spin-state Co^{3+}, indicating that the Co^{3+} matrix mainly keeps the LS state. However, the magnetization is not yet saturated at 7 T unlike that of the Cr-substituted sample, suggesting that the Mn substitution has a subtle but finite effect on the Co^{3+} matrix. We discuss this point in Sec. IV C.

The magnetization curves for the Fe-substituted sample were close to the $S = 5/2$ Brillouin function, and no giant magnetic moment was observed, unlike that in the Sr-substituted system. Therefore, the Fe ion will be effectively magnetically isolated with $S = 5/2$ and the Co^{3+} LS state will be maintained. Further, unfilled e_g orbital leads to an instantaneously unfilled t_{2g} orbital state through a second perturbative excitation and de-excitation process, which is
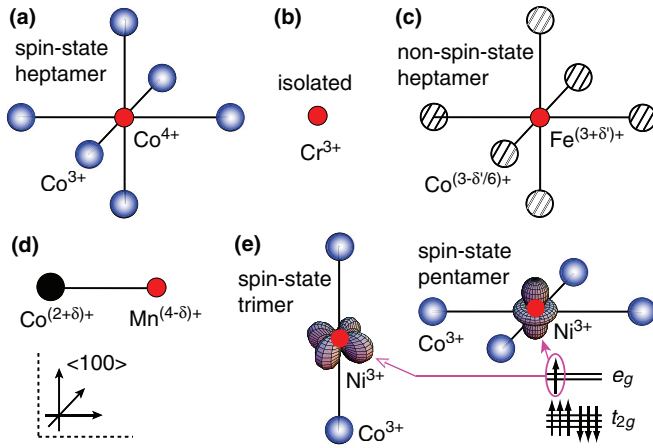
FIG. 6. (Color online) Models of system responses for light impurity substitutions in LaCoO$_3$. A small red solid circle denotes a magnetic impurity transition-metal ion or a doped hole (Co^{4+}), a gradational blue circle denotes a magnetic-spin-state Co^{3+} (IS or HS), a shaded circle denotes a LS Co$^{(3-\delta'/6)+}$ that is weakly magnetic because of δ', and a large black solid circle denotes HS Co$^{(2+\delta)+}$. The line between a transition-metal ion and a Co ion denotes a covalent bond between them through an oxygen anion located on the line. The oxygen and matrix nonmagnetic LS Co^{3+} ions are omitted in all the figures. (a) Heptamer model with spin-state change for Sr substitution (Co^{4+}) (Ref. [18]). (b) Magnetically isolated Cr^{3+} model. (c) Heptamer model without spin-state change for Fe substitution. (d) Model for Mn substitution. A part of valence might be located at oxygen as a hole (Ref. [26]). (e) Trimer and pentamer models for LS Ni^{3+} substitution with one $d_{x^2-y^2}$ electron and one $d_{3z^2-r^2}$ electron, respectively. The occupied e_g orbitals are depicted at the Ni positions.

accompanied by the l.[29,30] Thus, the observed anisotropy is again attributed to the l of Fe$^{(3+\delta')+}$ [$d^{5-\delta'}$, $S = (5-\delta')/2$] with unfilled e_g orbital (Fig. 1). Strictly speaking, however, the $S = (5-\delta')/2$ is inconsistent with the value of 5 μ_B observed at 7 T. Thus, it is considered that the δ' electron expands to the nearby O^{2-} and Co^{3+} (LS) ions by catalytically borrowing their orbitals, in a similar manner to what occurs in a complex or a molecule, but is still ferromagnetically coupled with the Fe spins, which behave magnetically as $S = 5/2$. Further, since all the $2p$ orbitals of O^{2-} are filled, the δ' electron is expected to be stable at Co^{3+} (LS) beyond O^{2-} and to generate a molecular ferromagnet without spin-state change, like the model shown in Fig. 6(c).

B. Ni substitution

For the Ni-substituted sample, the exact electronic state has been somewhat controversial so far; it could be trivalent or divalent and may depend on the Ni concentration and subtle sample synthesis conditions.[10,31–34] Thus, we discuss here three states: Ni^{3+} (LS), Ni^{3+} (HS), and the Ni^{2+} and Co^{4+} pair. First, Ni^{3+} (LS) is Jahn-Teller active with e_g orbital symmetry, which agrees with the observed [100] magnetic anisotropy. Second, in contrast to this, since Ni^{3+} (HS) is equivalent to Co^{2+} in terms of d^7 with l, anisotropy like that seen in the Mn-substituted sample magnetizations is expected, which is much smaller than the present Ni-substituted sample results.

Third, Ni^{2+} is isotropic without either Jahn-Teller activity or l, and the Co^{4+} should exhibit a giant magnetic moment of over 10 μ_B. Both of these are inconsistent with the Ni-substituted sample results. Thus, we conclude that the substituted Ni ion takes the trivalent LS state.

On the basis of this conclusion, since Ni^{3+} (LS) exhibits a moment of only 1 μ_B (Fig. 1), which is far below the experimental value of $\sim$6 μ_B at 7 T, its surrounding Co^{3+} ions change from LS to another magnetic spin state. Interestingly, in Ni^{3+} (LS), only one majority-spin e_g orbital is empty, unlike in Co^{4+} in which both majority-spin e_g orbitals are empty (hole doping). Therefore, based on the double exchange mechanism,[18] our experimental data suggests the emergence of *anisotropic* ferromagnetic spin-state clusters, that is, a bar magnet for the $d_{3z^2-r^2}$ empty orbital and a plane magnet for the $d_{x^2-y^2}$ empty orbital, as shown in Fig. 6(e).

At this stage, however, the magnetic-spin-state Co^{3+} cannot be identified as either IS, HS, or another possible spin state with noninteger e_g electrons. Also, the electronic states might be unique to the light substitution and are not necessarily maintained at higher Ni concentrations. These points should be studied in the future.

C. Factors to change the low-spin state in Co^{3+}

We thus now seek an answer to the question "what makes the Co^{3+} LS state change?" The present experimental results revealed that this change is almost completely absent for Cr or Fe substitution, is mainly absent for Mn or Co^{2+} (electron doping by Mn substitution) substitution, but does occur for Co^{4+} (hole doping by Sr substitution)[7] and Ni substitution. Interestingly, we note that Cr, Mn, and Fe are all lower group elements compared to Co and that Ni is in a higher group. This strongly suggests that a key factor is the chemical potential energy (Fermi energy or atomic orbital energy) of an outermost electron. For these elements, the energy is ordered as Cr > Mn > Fe > Co^{2+} > Co^{3+} > Co^{4+} > Ni with a $\sim$1 eV difference,[35,36] where the order of the Co ions is based on the Coulomb potentials. Thus, in the spin-state change, instead of losing excitation energy in changing from the t_{2g} to e_g orbital in Co^{3+}, an excited e_g-electron cloud flows slightly from the Co^{3+} to the impurity atom so as to lower the total energy not only through the kinetic double exchange (normally $<\sim$0.1 eV) but also through the lower chemical potential of the impurity atom ($\sim$1 eV).

The lattice strain and chemical pressure will also have an effect on the LS state change; magnetic spin (LS) states favor tensile (compressive) strain, as suggested by the existence of a pressure-induced spin-state transition.[5] Density functional calculations have also suggested that LaCoO$_3$ exhibits a HS/LS mixed state for tensile strain over a threshold value in magnitude, while the LS state is robust for compressive strain.[37] Thus, we here evaluate the threshold value of minimum ionic radius r_{min} of impurity atoms, above which the LS state does not completely change to HS state but begins to suffer a subtle effect for very light substitution. Table I summarizes the ionic radii r of the impurity atoms and matrix Co^{3+} in the literature.[38] First, nonmagnetic Al and Ga substitution maintains the LS state even at high concentration.[39] This Al ineffectiveness is consistent with the robustness of LS

TABLE I. Shannon ionic radii in descending order in Å units (Ref. [38]). The average value for dominant valence of $r_{Mn^{4+}}$ (0.53 Å) and $r_{Co^{2+}}$ (0.745 Å) for Mn substitution and $r_{Fe^{4+}}$ (0.585 Å) to $r_{Fe^{3+}}$ (0.645 Å) for Fe substitution are listed.

Ion	Radius	Ion	Radius
$r_{Rh^{3+}}$	0.665	$r_{Co^{3+}(HS)}$	0.61
r_{Mn}	0.638	$r_{Ni^{3+}(LS)}$	0.56
$r_{Ga^{3+}}$	0.62	$r_{Co^{3+}(LS)}$	0.545
$r_{Cr^{3+}}$	0.615	$r_{Al^{3+}}$	0.535
$r_{Fe^{(3+\delta')+}}$	0.615 ± 0.03		

state for compressive strain, whereas the Ga ineffectiveness indicates $r_{Ga^{3+}} < r_{min}$. Second, nonmagnetic Rh substitution barely maintains the LS state but exhibits an appreciably larger increase in magnetic susceptibility than the nonsubstituted system at a substitution level of only 2%.[40] Above 4%, the HS state with ferromagnetic correlations appears,[39–41] which was ascribed to the large $r_{Rh^{3+}}$ in other density functional calculations.[40] Thus, $r_{Rh^{3+}}$ is thought to exceed r_{min}. Third, in the present Mn-substituted sample magnetization data also, the absence of saturation suggests that the LS state is barely maintained but suffers a subtle effect, as mentioned in Sec. IV A. Further, other magnetization measurements detected slight sign of ferromagnetic correlations at a Mn substitution level of 5%,[42] which is also similar to those in the Rh-substituted system. Thus, the subtle effect is also attributed to strain and r_{Mn} will be beyond r_{min}. In this way, we obtain $r_{min} \simeq 0.63 \pm 0.01$ Å as a value between $r_{Ga^{3+}}$ and r_{Mn}. This value is obviously larger than $r_{Co^{3+}(HS)}$, which is in agreement with the HS state appearance model.

As discussed above, the overall trend in the present data can be explained by the ionic picture. In fact, for Cr substitution, since the present data indicates the magnetically isolated Cr^{3+}, a Cr^{3+}-O-Co^{3+} (LS) bond is most probably ionic. For other substitution, however, it is considered that covalency between transition-metal cations through oxygen anions supports the observed Co-matrix responses to impurity substitution. For Ni substitution, since double exchange between Ni^{3+}-O-Co^{3+} (magnetic spin state) will generate the spin-state molecular ferromagnets, as shown in Fig. 6(e), high covalency or molecular orbital is expected to be formed in the magnet. This is analog with the Sr-substituted (hole-doped) system with similar spin-state molecular ferromagnets, accompanied by double-exchange-driven high covalency between Co^{4+}-O-Co^{3+} (IS).[18] Further, since Fe substitution also induces another type of molecular ferromagnet as in Fig. 6(c), high covalency is expected for the δ' electron expanding in the magnet. For Mn substitution, earlier x-ray absorption spectroscopy studies for a wide Mn concentration range suggested the Mn^{3+}/Mn^{4+}-O-Co^{2+}/Co^{3+} mixed valence state with superexchange interaction and a $d^7\underline{L}$ state for mixed valence Co^{2+}/Co^{3+}.[24,26,43] Such covalency will be also the case for the present light Mn substitution.

The LS state responses to Cr, Mn, Fe, Ni, Al, Ga, and Rh substitution are summarized as follows. Ni substitution will sensitively induce magnetic-spin-state Co^{3+} via the chemical potential combined with double exchange and high covalency. Rh and Mn substitution will gradually induce magnetic-spin-

state Co^{3+} via strain in accordance with a substitution level and magnitude of magnetic field. All other substitution without a low chemical potential or a large ionic radius will maintain the LS state of Co^{3+}.

D. Applications of the present results

We discuss applications of the present results on the d^6 LS state change in $LaCoO_3$. One example of the application is impurity effects for the Earth's most abundant phase, perovskite (Mg, Fe)(Si, Al)O_3. The Fe atoms take divalent d^6 states, and change from HS towards LS states with increasing mantle depth and pressure.[44] Interestingly, this spin-state change is suppressed in lightly Al-substituted $(Mg_{0.86}Fe_{0.14})(Si_{0.98}Al_{0.02})O_3$ compared to $(Mg_{0.88}Fe_{0.12})SiO_3$.[44] Although the physical origin has not been clarified thus far probably because of experimental difficulty under extremely high pressure, the present results provide the following interpretation. The Al^{3+} substitution of Si^{4+} corresponds to the hole doping to Fe sites like the Sr^{2+} substitution of La^{3+}. The Fe^{2+} LS state change will be therefore significant via the chemical potential with approaching the LS state, which is attributable to the origin. Furthermore, Al^{3+} is much larger than Si^{4+} (0.400 Å),[38] which will be also the origin.

Another example of the application is impurity effects for pyrite FeS_2, in which Fe is also described by the same nonmagnetic LS state $[d^6: (t_{2g})^6, (e_g)^0, 0\,\mu_B]$[45] For the Fe-site substitutions, the matrix Fe LS state does not change for Mn $[d^5: (t_{2g})^3, (e_g)^2, 5\,\mu_B]$ or Ni $[d^8: (t_{2g})^6, (e_g)^2, 2\,\mu_B]$ substitution[46,47] but does sensitively change for Co $[d^7: (t_{2g})^6, (e_g)^1, 1]$ substitution, only 1% of which leads to a ferromagnetic phase.[48] This chemical trend is consistent with the present picture as follows. The Mn ineffectiveness will occur since Mn is a lower group element with higher chemical potential energy compared to Fe, which is similar to Fe-doped $LaCoO_3$. The Ni ineffectiveness will occur since all the Ni majority-spin orbitals are filled, which forbids the double exchange. In contrast, the Co effectiveness will correspond to the lightly Ni-substituted $LaCoO_3$ with ferromagnetic spin-state clusters.

V. SUMMARY

In summary, we have studied the impurity-induced spin-state responses in lightly substituted single crystals of $LaCo_{0.99}M_{0.01}O_3$ (M = Cr, Mn, Fe, Ni) using magnetization, x-ray fluorescence, and electrical resistivity measurements. A distinct spin-state change from the LS state in Co^{3+} was observed only in the Ni-substituted sample, which was accompanied by strong magnetic anisotropy. This change, which has been demonstrated experimentally for the first time, suggests the emergence of *anisotropic* ferromagnetic spin-state clusters as the expanded model of a spin-state heptamer generated by hole doping. Further, the results of the present experiments suggest that the chemical potential is also a key factor in the spin-state transition, in addition to the temperature, magnetic field, pressure (strain), and double exchange mechanism. For the strain-driven spin-state responses, the threshold minimum ionic radius of a lightly substituted impurity was evaluated. Taking for example mantle

materials and impurity-substituted pyrites with Fe, which has the same d^6 spin-state degree of freedom as the Co^{3+} in $LaCoO_3$, we also discussed applications of the present results. In future, nuclear magnetic resonance (NMR) and soft x-ray experiments could provide the detailed local electronic information on impurity atoms and their surroundings.

*tomiyasu@m.tohoku.ac.jp

[1] R. R. Heikes, R. C. Miller, and R. Mazelsky, Physica **30**, 1600 (1964).

[2] V. G. Bhide, D. S. Rajoria, G. R. Rao, and C. N. R. Rao, Phys. Rev. B **6**, 1021 (1972).

[3] K. Asai, P. Gehring, H. Chou, and G. Shirane, Phys. Rev. B **40**, 10982 (1989).

[4] K. Sato, A. Matsuo, K. Kindo, Y. Kobayashi, and K. Asai, J. Phys. Soc. Jpn. **78**, 093702 (2009).

[5] K. Asai, O. Yokokura, M. Suzuki, T. Naka, T. Matsumoto, H. Takahashi, N. Môri, and K. Kohn, J. Phys. Soc. Jpn. **66**, 967 (1997).

[6] M. A. Korotin, S. Y. Ezhov, I. V. Solovyev, V. I. Anisimov, D. I. Khomskii, and G. A. Sawatzky, Phys. Rev. B **54**, 5309 (1996).

[7] S. Yamaguchi, Y. Okimoto, H. Taniguchi, and Y. Tokura, Phys. Rev. B **53**, R2926 (1996).

[8] M. Kriener, C. Zobel, A. Reichl, J. Baier, M. Cwik, K. Berggold, H. Kierspel, O. Zabara, A. Freimuth, and T. Lorenz, Phys. Rev. B **69**, 094417 (2004).

[9] G. H. Jonker, J. Appl. Phys. **37**, 1424 (1966).

[10] D. Hammer, J. Wu, and C. Leighton, Phys. Rev. B **69**, 134407 (2004).

[11] R. Robert, M. H. Aguirre, L. Bocher, M. Trottmann, S. Heiroth, T. Lippert, M. Döbeli, and A. Weidenkaff, Solid State Sci. **10**, 502 (2008).

[12] D. V. Karpinsky, I. O. Troyanchuk, K. Bärner, H. Szymczak, and M. Tovar, J. Phys.: Condens. Matter **17**, 7219 (2005).

[13] D. V. Karpinsky, I. O. Troyanchuk, V. M. Dobryansky, R. Szymczak, and M. Tovar, Crystallogr. Rep. **51**, 596 (2006).

[14] D. V. Karpinsky, I. O. Troyanchuk, and M. Kopcewicz, Phys. Status Solidi B **244**, 1409 (2007).

[15] S. Yamaguchi, Y. Okimoto, and Y. Tokura, Phys. Rev. B **55**, R8666 (1997).

[16] D. Louca and J. L. Sarrao, Phys. Rev. Lett. **91**, 155501 (2003).

[17] D. Phelan, D. Louca, K. Kamazawa, S. H. Lee, S. Rosenkranz, M. F. Hundley, J. F. Mitchell, Y. Motome, S. N. Ancona, and Y. Moritomo, Phys. Rev. Lett. **97**, 235501 (2006).

[18] A. Podlesnyak, M. Russina, A. Furrer, A. Alfonsov, E. Vavilova, V. Kataev, B. Büchner, T. Strässle, E. Pomjakushina, K. Conder *et al.*, Phys. Rev. Lett. **101**, 247603 (2008).

[19] A. Podlesnyak, G. Ehlers, M. Frontzek, A. S. Sefat, A. Furrer, T. Strässle, E. Pomjakushina, K. Conder, F. Demmel, and D. I. Khomskii, Phys. Rev. B **83**, 134430 (2011).

[20] The spin-state polarons are classified into magnetic polarons with spontaneous magnetization, not into normal polarons with electric polarization.

[21] M. Itoh, I. Natori, S. Kubota, and K. Motoya, J. Phys. Soc. Jpn. **63**, 1486 (1994).

[22] J. Wu and C. Leighton, Phys. Rev. B **67**, 174408 (2003).

[23] B. G. Tilset, H. Fjellvåg, A. Kjekshus, and B. C. Hauback, Acta Chem. Scand. **52**, 733 (1998).

[24] M. Sikora, C. Kapusta, K. Knížek, Z. Jirák, C. Autret, M. Borowiec, C. J. Oates, V. Procházka, D. Rybicki, and D. Zajac, Phys. Rev. B **73**, 094426 (2006).

[25] S. R. English, J. Wu, and C. Leighton, Phys. Rev. B **65**, 220407(R) (2002).

[26] J. van Elp, Phys. Rev. B **60**, 7649 (1999).

[27] J. R. Singer, Phys. Rev. **104**, 929 (1956).

[28] G. Blasse, J. Phys. Chem. Solids **26**, 1969 (1965).

[29] S. Ohtani, Y. Watanabe, M. Saito, N. Abe, K. Taniguchi, H. Sagayama, T. Arima, M. Watanabe, and Y. Noda, J. Phys.: Condens. Matter **22**, 176003 (2010).

[30] H. Sagayama, S. Ohtani, M. Saito, N. Abe, K. Taniguchi, and T. Arima, Appl. Phys. Lett. **99**, 082506 (2011).

[31] C. N. R. Rao, O. Parkash, and P. Ganguly, J. Solid State Chem. **15**, 186 (1975).

[32] Y. Kobayashi, S. Murata, K. Asai, J. M. Tranquqda, G. Shirane, and K. Kohn, J. Phys. Soc. Jpn. **68**, 1011 (1999).

[33] S. Ivanova, A. Senyshyn, E. Zhecheva, K. Tenchev, R. Stoyanova, and H. Fuess, J. Solid State Chem. **183**, 940 (2010).

[34] J. Yu, K. Kamazawa, and D. Louca, Phys. Rev. B **82**, 224101 (2010).

[35] R. Latter, Phys. Rev. **99**, 510 (1955).

[36] T. Ishii, S. Tsuboi, G. Sakane, M. Yamashita, and B. K. Breedlove, Dalton Trans. (2009) 680.

[37] H. Seo, A. Posadas, and A. A. Demkov, Phys. Rev. B **86**, 014430 (2012).

[38] R. D. Shannon, Acta Crystallogr. **A32**, 751 (1976).

[39] T. Kyômen, Y. Asaka, and M. Itoh, Phys. Rev. B **67**, 144424 (2003).

[40] K. Knížek, J. Hejtmánek, M. Maryško, Z. Jirák, and J. Buršík, Phys. Rev. B **85**, 134401 (2012).

[41]S. Asai, N. Furuta, Y. Yasui, and I. Terasaki, J. Phys. Soc. Jpn. **80**, 104705 (2011).

[42]C. Autret, J. Hejtmánek, K. Knížek, M. Maryško, Z. Jirák, M. Dlouhá, and S. Vratislav, J. Phys.: Condens. Matter **17**, 1601 (2005).

[43]J.-H. Park, S.-W. Cheong, and C. T. Chen, Phys. Rev. B **55**, 11072 (1997).

[44]C. McCammon, I. Kantor, O. Narygina, J. Rouquette, U. Ponkratz, I. Sergueev, M. Mezouar, V. Prakapenka, and L. Dubrovinsky, Nat. Geosci. **1**, 684 (2008).

[45]W. Folkerts, G. A. Sawatzky, C. Haas, R. A. de Groot, and F. U. Hillebrecht, J. Phys. C: Solid State Phys. **20**, 4135 (1987).

[46]K. Adachi, K. Sato, S. Kubo, and K. Yamauchi, J. Phys. Soc. Jpn. **30**, 577 (1971).

[47]K. Adachi, T. Ueno, M. Tohda, and H. Sawamoto, J. Phys. Soc. Jpn. **41**, 1069 (1976).

[48]S. Guo, D. P. Young, R. T. Macaluso, D. A. Browne, N. L. Henderson, J. Y. Chan, L. L. Henry, and J. F. DiTusa, Phys. Rev. Lett. **100**, 017209 (2008).